Regular Article

PHYSICAL CHEMISTRY RESEARCH
Published by the
Iranian Chemical Society
www.physchemres.org
info@physchemres.org

Phys. Chem. Res., Vol. 9, No. 2, 311-325, June 2021
DOI: 10.22036/pcr.2021.247509.1830

ZnO-$MgFe_2O_4$/(Mg)- or (Zn)-Al-LDH Composites: Adsorption Efficiency, Kinetics, and Adsorption Isotherm for Congo Red Removal

P. Yarahmadi, M. Movahedi* and H. Salavati

Department of Chemistry, Payame Noor University, P. O. Box: 19395-3697 Tehran, Iran

(Received 9 September 2020, Accepted 26 February 2021)

In this research, ZnO-$MgFe_2O_4$/ZnAl-LDH, ZnO-$MgFe_2O_4$/MgAl-LDH, ZnO-$MgFe_2O_4$, ZnAl-LDH and MgAl-LDH were prepared and characterized using X-ray diffraction (XRD), field emission scanning electron microscopy (FE-SEM), and FT-IR spectrometer analyses. The samples were synthesized by the co-precipitation method. The efficiency of the samples was investigated for the Congo red dye removal from the aqueous solution. According to the results, a similar efficiency for the LDHs samples and ZnO-$MgFe_2O_4$/LDHs composites was observed. The experimental data for the ZnO-$MgFe_2O_4$/ZnAl-LDH and ZnO-$MgFe_2O_4$/MgAl-LDH composites were analyzed by adsorption isotherm (Langmuir and Freundlich) and kinetic models (pseudo-first-order, pseudo-second-order, and intra-particle diffusion). The results showed that more than >90% of the Congo red dye was removed from the solution after 90 min contact time. The experimental results showed the adsorption process fitted well with the Langmuir isotherm model and pseudo-second-order kinetic model. For the ZnO-$MgFe_2O_4$/ZnAl-LDH and ZnO-$MgFe_2O_4$/MgAl-LDH samples, the R_L value close to zero (0.024 and 0.037) was obtained. This result indicates that the adsorption of the CR dye molecules on the surface of the samples is an almost irreversible process. The low R_L value indicates that the interactions between Congo red dye molecules and LDH composites might be relatively strong.

Keywords: ZnO-$MgFe_2O_4$, ZnAl-LDH, MgAl-LDH, Adsorbent, Composite

INTRODUCTION

Different methods are employed to reduce hazardous organic and inorganic pollutants from effluents. Most of organic dyes are highly dissolved in aqueous solutions, they are very toxic, mutagenic and carcinogenic, causing serious damage to the environment and human beings. Congo red dye is used in textile, plastic, rubber and paper industries, and consequently found in their wastewater [1,2]. The adsorption method is preferred for the treatment of the wastewater due to its low cost, simple design, and easy operation. Until now different types of natural and synthetic adsorbents such as clays, biosorbents, industrial by-products, agricultural solid wastes, and composites are used for dye removal from aqueous solution [3,4]. In recent years, many composite materials and modified adsorbents have been synthesized to improved adsorption performance [5]. Layered double hydroxides (LDHs) are used as adsorbents to remove dyes and heavy metals. LDHs are favored due to facility synthesis, low toxicity, high stability, and low cost [6,7]. LDHs are known as hydrotalcite-like compounds. LDHs have layered structure with formula $[M^{+2}_{(1-x)}M^{+3}(OH)_2]^{X+}(A^{n-})_{x/n}.mH_2O$ where M^{2+} and M^{3+} represent bivalent and trivalent cations respectively, while, A^{n-} are interlayer anions. LDH is a clay material consisting of a positively charged metal hydroxide sheet with intercalated anions and water molecules. Hence, LDHs are good candidates for anionic dye removal because of the surface complexation and electrostatic interactions [8,9]. Many researchers have reported that the combination of LDHs with other material such as polymers, magnetic materials, clay, semiconductors and surfactants significantly

*Corresponding author. E-mail: m.movahedi@pnu.ac.ir

improves the surface characteristics, and adsorption performance [10-14]. Preparation of magnetic adsorbent has developed recently to enhance separation of adsorbent from aqueous solution. Magnetic adsorbents can be easily separated and reused by an external magnetic field. Today, ferrite spinel composites are used for this purpose [15]. Until now, various composites based on ferrite and LDH such as $CoFe_2O_4$/CuAl-LDH, $NiFe_2O_4$/ZnCuCr-LDH, Fe_3O_4@MgAl-LDH, Fe_3O_4/Zn-Al-Fe-La-LDH and Fe_3O_4/ZnCr-LDH have been reported [16-20]. The aim of this research was the preparation and comparison of the ZnO-$MgFe_2O_4$/ZnAl-LDH and ZnO-$MgFe_2O_4$/MgAl-LDH samples for Congo red dye removal from the aqueous solution. The sorption kinetics and isotherms were also investigated.

EXPERIMENTAL

Materials

Congo red dye, $Zn(OAc)_2.2H_2O$, $Mg(NO_3)_2.4H_2O$, $Fe(NO_3)_3.9H_2O$, $MgCl_2.6H_2O$, $AlCl_3.6H_2O$, $Zn(NO_3)_2.6H_2O$, $Al(NO_3)_2.9H_2O$ and NaOH (purity ≥ 98%) were purchased from Sigma-Aldrich and Merck Company.

Instrumentation

To characterize the samples, different equipment such as XRD (Holland Philips Xpert, X-ray diffractometer with Cu-Kα radiation), field emission scanning electron microscopy (FE-SEM, Vega 2 Tscan), UV-Vis. spectrophotometer (Shimadzu-2550), and FT-IR spectrometer (JASCO-4200) were employed.

Preparation of ZnO-$MgFe_2O_4$ Composite

Initially, $Zn(OAc)_2.2H_2O$ (2.19 g) was dissolved in 150 ml distilled water. Then, 15 ml of the NaOH solution (4 M) was added and sonicated for 15 min. After that, 50 ml of the aqueous solution containing $Mg(NO_3)_2.4H_2O$ (0.22 g) and $Fe(NO_3)_3.9H_2O$ (0.808 g) was added into the above suspension and sonicated for 30 min. The final precipitate was separated and washed with distilled water several times and dried in an oven at 70 °C for 24 h. Finally, the prepared sample was calcined at 800 °C for 1 h.

Preparation of ZnAl- and MgAl-LDHs

The co-precipitation method was employed for the synthesis of the layered double hydroxides [21]. For preparation of ZnAl-LDH, 2.97 g of $Zn(NO_3)_2.6H_2O$ and 1.88 g of $Al(NO_3)_3.9H_2O$ (Zn^{2+}/Al^{3+}, mole ratio 2:1) were dissolved in 100 ml double distilled water and pH of the solution was adjusted to 9 by adding NaOH (4 M) solution. The precipitate formed was aged at 80 °C for 24 h. The resulting precipitate was collected by centrifuge, rinsed with distilled water many times and dried in an oven at 60 °C. The MgAl-LDH (Mg^{2+}/Al^{3+}, mole ratio 2:1) was synthesized using Mg^{2+} and Al^{3+} chloride salts.

Preparations of ZnO-$MgFe_2O_4$/LDH Composites

The preparation of ZnO-$MgFe_2O_4$/LDH was carried out by adding the ZnO-$MgFe_2O_4$ sample during the synthesis of the layered double hydroxide. First, 0.2 g of the prepared ZnO-$MgFe_2O_4$ was dispersed in 50 ml of distilled water and added to a solution containing metal salts under vigorous stirring. Next, NaOH solution was added dropwise, and then the reaction mixture was heated at 80 °C for 24 h. Finally, the product was washed several times and dried in an oven at 60 °C.

Adsorption Kinetic

Typically, 0.1 g of the samples was added into the 200 ml CR dye solution (18, 52, 72 mg l^{-1}). After contact times of 15, 30, 45, 60, 90, 120 and 180 min, the CR dye concentration was measured by a UV-Vis. spectrophotometer. The adsorption capacity and dye removal percentage were calculated according to Eqs. (1) and (2), respectively [22,23],

$$Adsorption\,capacity\,(q_t) = \frac{(C_0 - C_t)\,V}{m} \times 100 \quad (1)$$

$$Dye\,removal\,(\%) = \frac{C_0 - C_t}{C_0} \times 100 \quad (2)$$

where C_0 (mg l^{-1}) and C_t (mg l^{-1}) are initial dye concentration and dye concentration at time t, V (l) and m (g) are volume of the dye solution and adsorbent mass, respectively.

The adsorption behavior of CR onto the prepared samples was analyzed by using the pseudo-first-order, pseudo-second-order and intera-particle diffusion models

[24] by the following Eqs. ((3)-(5)),

$$\ln(q_e - q_t) = \ln q_e - k_1 t \quad (3)$$

$$\frac{t}{q_t} = \frac{1}{k_2 q_e^2} + \frac{t}{q_e} \quad (4)$$

$$q_t = k_{id} t^{0.5} + C \quad (5)$$

where k_1, k_2 and k_{id} are the rate constants, q_e and q_t are the amounts of adsorption (mg g^{-1}) at equilibrium and at time t, respectively.

Adsorption Isotherm

The adsorption isotherms of the ZnO-$MgFe_2O_4$/ZnAl-LDH and ZnO-$MgFe_2O_4$/MgAl-LDH samples were investigated using Langmuir and Freundlich models. The Langmuir isotherm model is given as Eq. (6) [25],

$$\frac{C_e}{q_e} = \frac{1}{q_{\max} K_L} + \frac{C_e}{q_{\max}} \quad (6)$$

where q_{max} is the maximum adsorption capacity (mg g^{-1}), and K_L is the Langmuir constant. The essential characteristics of Langmuir isotherm can be expressed by a dimension less constant called separation factor (R_L) which is defined by Eq. (7). R_L indicates the adsorption nature, where unfavorable $R_L > 1$, linear $R_L = 1$, favorable $0 < R_L < 1$, and irreversible $R_L = 0$.

$$R_L = \frac{1}{1 + K_L C_0} \quad (7)$$

The Freundlich model is given as Eq. (8), where K_F is Freundlich constant ((mg g^{-1}) (l $mg^{-1})^{1/n}$) and n is a heterogeneity factor [26].

$$\ln q_e = \ln K_F + \frac{1}{n} \ln C_e \quad (8)$$

RESULTS AND DISCUSSION

Characterization

The XRD, FE-SEM and FT-IR analyses were used for characterization of the samples. For the ZnO-$MgFe_2O_4$ sample, the presence of zinc oxide (JCPDS card no. 80-0075) and $MgFe_2O_4$ (JCPDS card no. 88-1942) were confirmed by XRD pattern (Fig. 1a). The XRD pattern of the ZnO-$MgFe_2O_4$/ZnAl-LDH and ZnO-$MgFe_2O_4$/MgAl-LDH samples is shown in Figs. 1b and 1c, respectively. The ZnAl-LDH and MgAl-LDH samples were characterized by FT-IR spectra (Fig. 1d). The broad band at 3425 cm^{-1} and 3452 cm^{-1} corresponds to the hydroxyl groups and water molecules. For the ZnAl-LDH and MgAl-LDH samples the sharp vibration band at 1380 cm^{-1} and 1370 cm^{-1} can be assigned to interlayer NO_3^- and CO_3^{2-} anions, respectively [27]. During the synthesis of MgAl-LDH, the Cl^- and CO_3^{2-} ions competed. The interlayer chlorine bands are not observed in FT-IR spectrum of MgAl-LDH [28]. The lattice stretching and bending vibration ascribed to O-M and O-M-O bands for the ZnAl-LDH and MgAl-LDH were observed at (425, 608, 774) cm^{-1} and (440, 664, 770) cm^{-1}, respectively [29].

The morphology of the ZnAl-LDH (nanosheet), MgAl-LDH (nanoparticle), ZnO-$MgFe_2O_4$/ZnAl-LDH (nanosheet), ZnO-$MgFe_2O_4$/MgAl-LDH (nanoflake), ZnO-$MgFe_2O_4$ (nanoparticle and nanosheet) samples were investigated by FE-SEM images (Figs. 2a-e). According to the images, the particles' thickness at about 20 to 80 nm were estimated.

Adsorption Study

The experiments were conducted with different initial concentrations of CR (18, 52 and 72 mg l^{-1}) in the presence of 0.5 (g l^{-1}) of the adsorbent (ZnAl-LDH, MgAl-LDH, ZnO-$MgFe_2O_4$/ZnAl-LDH and ZnO-$MgFe_2O_4$/MgAl-LDH). The results showed that all adsorbents can effectively remove more than >90% of the CR dye and adsorption equilibrium occurred during (90-180) min contact time (Figs. 3a-d).

For all the samples, the adsorption capacity was calculated. The adsorption capacities of the ZnAl-LDH, MgAl-LDH, ZnO-$MgFe_2O_4$/ZnAl-LDH and ZnO-$MgFe_2O_4$/MgAl-LDH samples for CR dye removal with initial concentrations 18, 52 and 72 mg l^{-1}, respectively, were (35, 101, 139 mg g^{-1}), (35, 101, 140 mg g^{-1}), (35, 101, 130 mg g^{-1}) and (35, 99, 133 mg g^{-1}). The results showed that all the samples had almost a similar adsorption

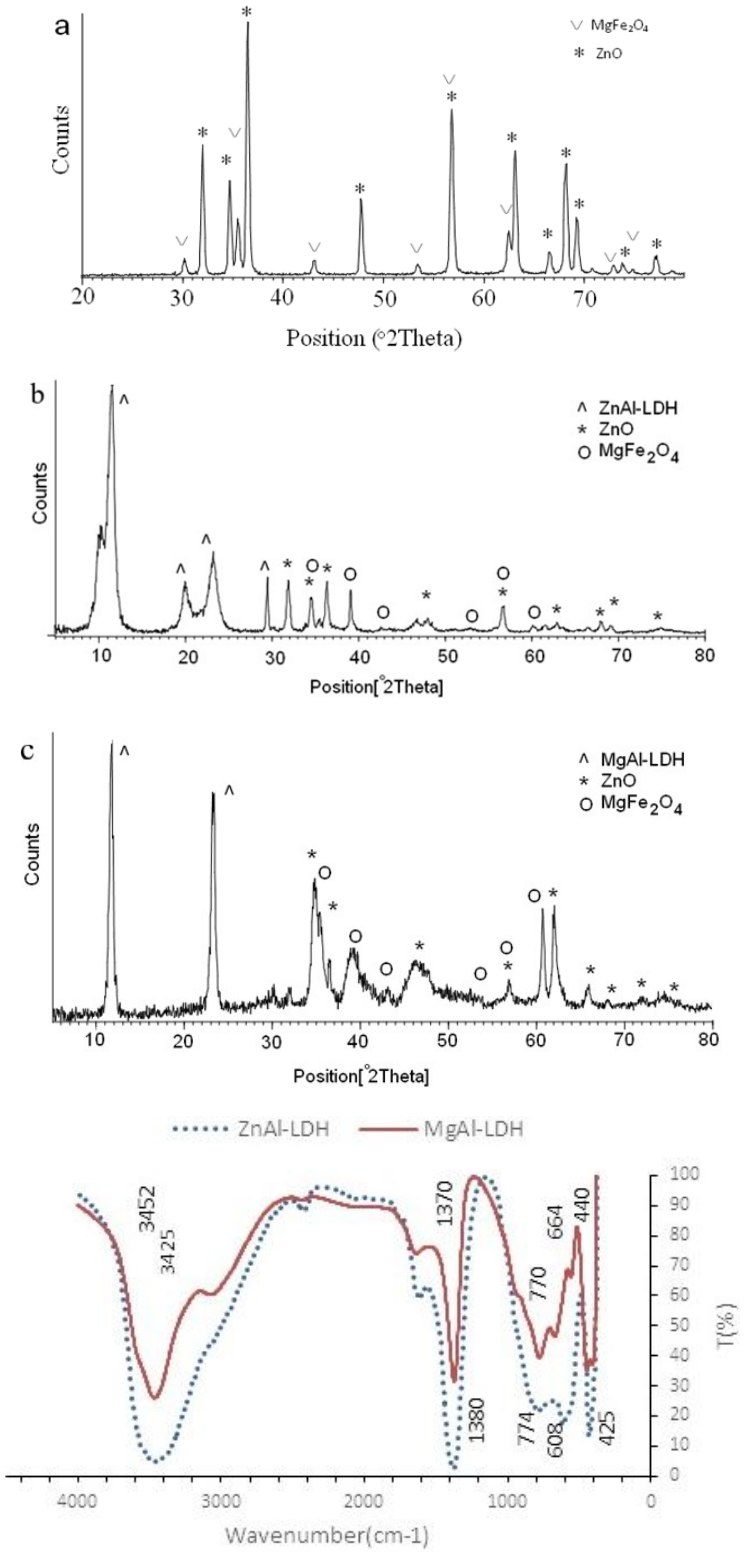

Fig. 1. XRD pattern of the (a) ZnO-$MgFe_2O_4$ composite, (b) ZnO-$MgFe_2O_4$/ZnAl-LDH, (c) ZnO-$MgFe_2O_4$/MgAl-LDH and (d) FT-IR spectra of the ZnAl-LDH and MgAl-LDH.

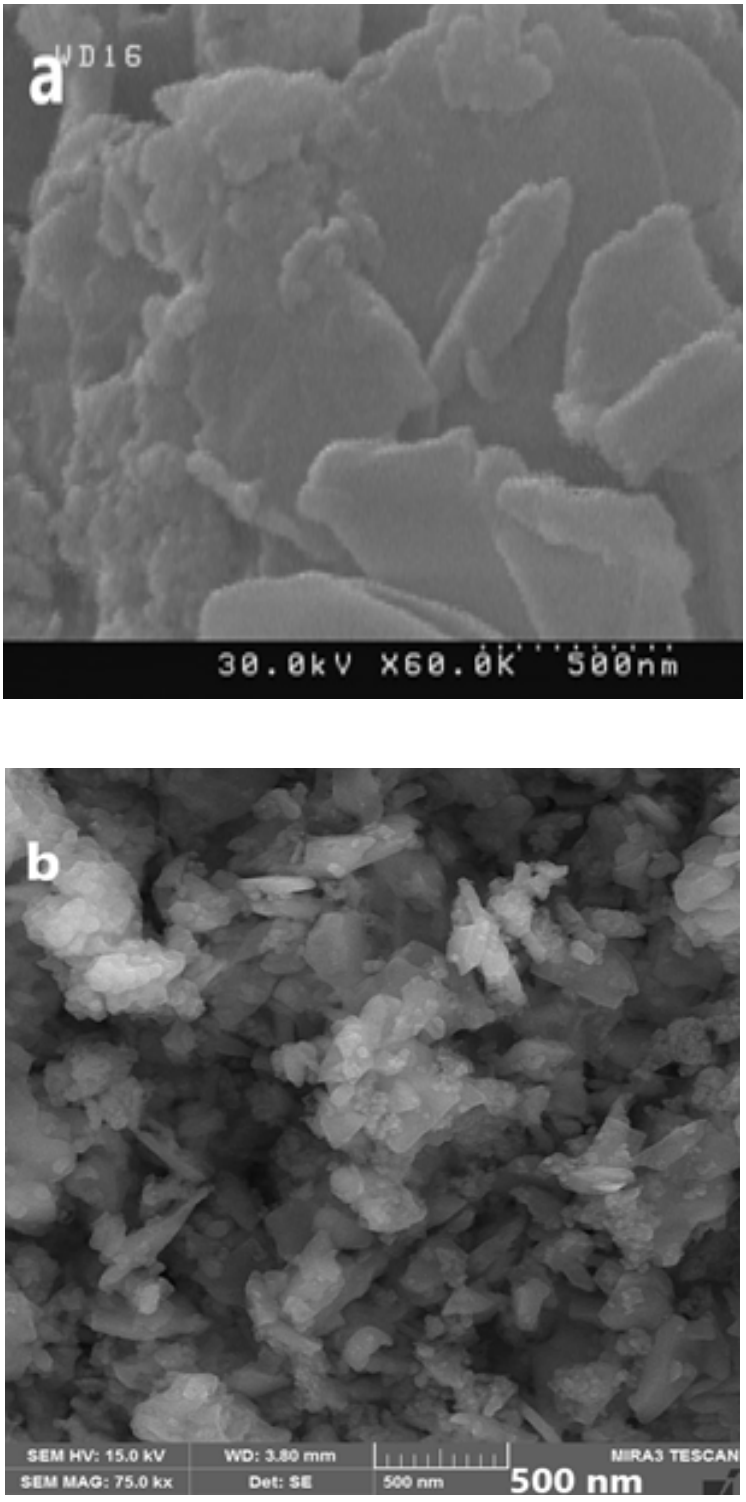

Fig. 2. FE-SEM images of (a) ZnAl-LDH, (b) MgAl-LDH, (c) ZnO-$MgFe_2O_4$/ZnAl-LDH, (d) ZnO-$MgFe_2O_4$/MgAl-LDH and (e) ZnO-$MgFe_2O_4$.

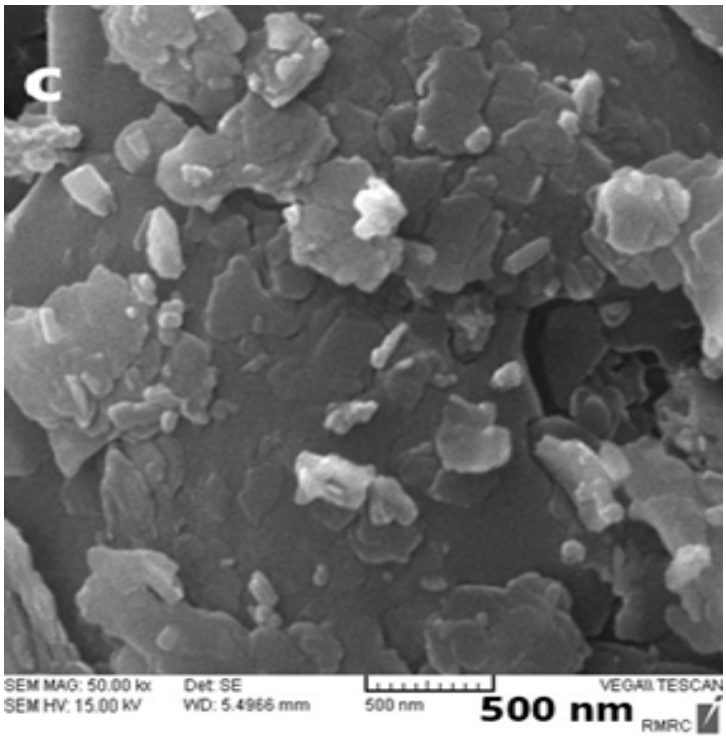

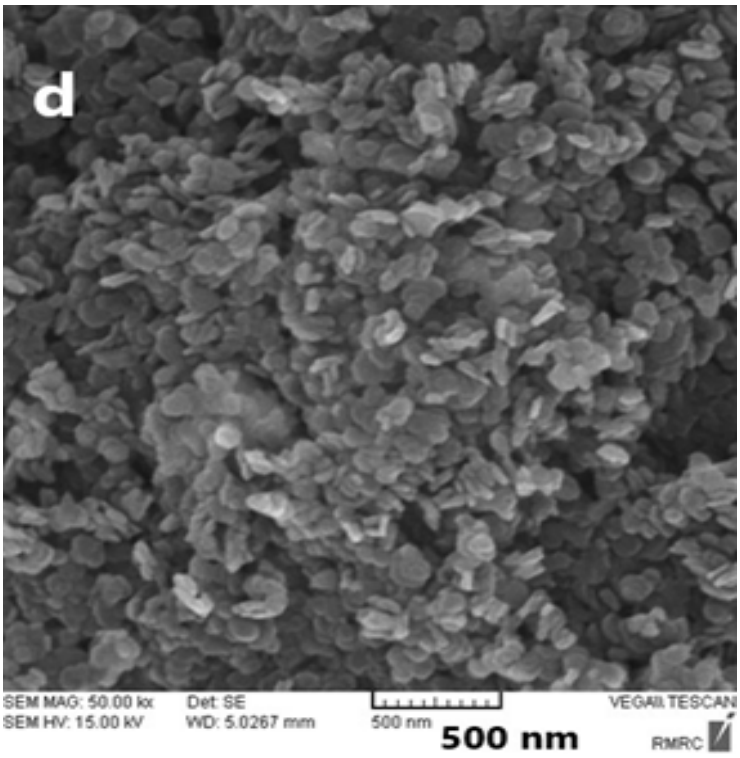

Fig. 2. Continued.

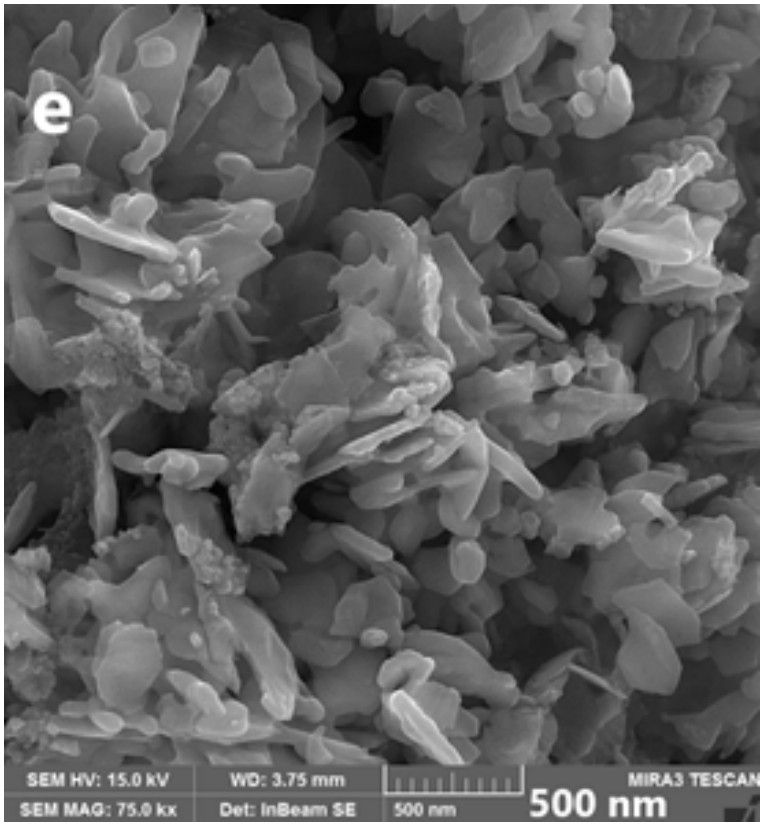

Fig. 2. Continued.

capacity. Moreover, Figs. 4a-d shows the effect of contact time and dye concentration on the adsorption capacity. According to the results, in the first stages of adsorption, the CR dye is rapidly adsorbed on the surface, then slowly increases with increasing time, and becoming almost constant after 90 min. With increasing initial dye concentration, more molecules are adsorbed on the unoccupied sites of the adsorbent surface, and as result, the adsorption capacity increases with increasing concentration [30].

In another experiment, the adsorption capacity of the ZnO-$MgFe_2O_4$ sample as magnetic component was investigated. The adsorption capacity value of 60 mg g^{-1} was obtained for the ZnO-$MgFe_2O_4$ sample. The maximum adsorption capacities of the samples were compared with those of other LDHs and magnetic adsorbents reported in the literature (Table 1).

The kinetic behavior of the dye adsorption process onto the ZnO-$MgFe_2O_4$/ZnAl-LDH and ZnO-$MgFe_2O_4$/MgAl-LDH samples was analyzed by using the pseudo-first-order, pseudo-second-order and intra-particle diffusion models (Figs. 5a-f). The results showed the sorption process follow a pseudo-second-order kinetic model (Table 2). The pseudo-second-order kinetic model and possibility of Congo red dye removal through chemisorption was reported by many researchers [31,32]. Furthermore, the results showed that the pseudo-second-order rate constant (k_2) decreases with increasing dye concentration (Table 2). These results showed that surface saturation was dependent to the initial dye concentration. Therefore, at low dye concentrations, dye molecules are rapidly adsorbed by the surface sites, and at high concentrations, dye molecules need to penetrate internal sites by intra-particle diffusion, and therefore the rate of adsorption decreases [30]. Furthermore, the results indicated that parameters of rate constant (k_2) and adsorption capacity (q_{e2}) depend on the initial CR dye

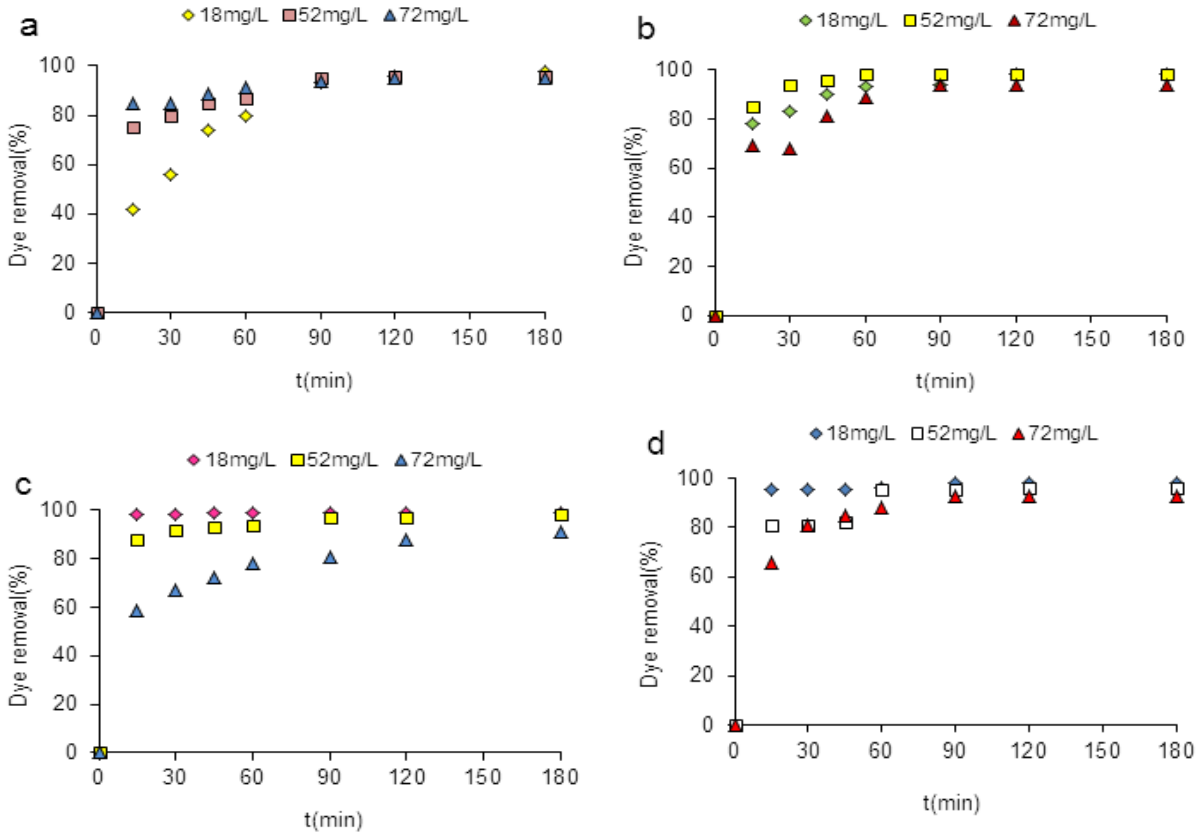

Fig. 3. Percentage of the CR dye removal by adsorbents; (a) ZnAl-LDH, (b) MgAl-LDH, (c) ZnO-$MgFe_2O_4$/ZnAl-LDH and (d) ZnO-$MgFe_2O_4$/MgAl-LDH.

Table 1. Comparative of Maximum Adsorption Capacity of Different Adsorbents for CR Dye Removal

Name of adsorbent	C_0 (mg l^{-1})	q_{max}	Ref.
Mg-Fe-CO_3-LDH	100	104.6	[38]
Cu-Mg-Al-LDH	20	44.5	[39]
CaAl-LDH	50	72.56	[40]
Fe_3O_4/MgAl-LDH	200	132	[11]
γ-Fe_2O_3/Sep-NH_2	70	117.7	[41]
Cellulose/Fe_3O_4/activated carbon	50	40.85	[42]
ZnAl-LDH	52	101	This work
MgAl-LDH	52	101	This work
ZnO-$MgFe_2O_4$/ZnAl-LDH	52	101	This work
ZnO-$MgFe_2O_4$/MgAl-LDH	52	99	This work
ZnO-$MgFe_2O_4$	52	60	This work

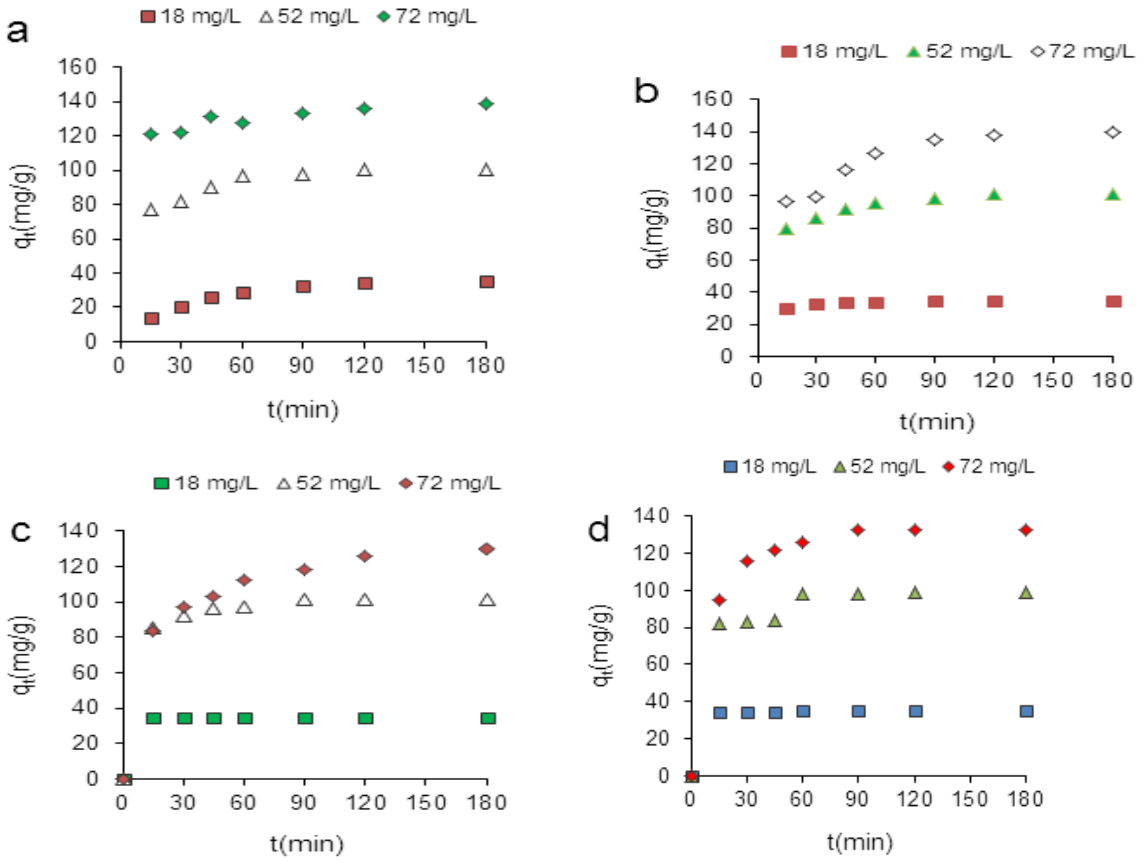

Fig. 4. Adsorption capacity of the adsorbents (a) ZnAl-LDH, (b) MgAl-LDH, (c) ZnO-$MgFe_2O_4$/ZnAl-LDH and (d) ZnO-$MgFe_2O_4$/MgAl-LDH for CR dye removal from aqueous solution (18, 52 and 72 mg l^{-1}).

Table 2. Pseudo-first-order and Pseudo-second-order Kinetic Parameters for Adsorption of CR onto the ZnO-$MgFe_2O_4$/ZnAl-LDH and ZnO-$MgFe_2O_4$/MgAl-LDH Adsorbents

Sample	C_0	q_e^{exp}	Pseudo-first order			Pseudo-second order		
			K_1 (min^{-1})	q_{e1} (mg g^{-1})	R^2	K_2 (g mg^{-1} min^{-1})	q_{e2} (mg g^{-1})	R^2
ZnO-$MgFe_2O_4$/ZnAl-LDH	18	35	8×10^{-5}	1.01	0.5048	9.14×10^{-2}	35.5	0.9996
	52	101	9×10^{-4}	1.12	0.5966	2.68×10^{-3}	103.1	0.9998
	72	130	22×10^{-4}	1.34	0.7579	6.52×10^{-4}	135.1	0.9986
ZnO-$MgFe_2O_4$/MgAl-LDH	18	35	2×10^{-4}	1.02	0.5836	4.44×10^{-2}	35.3	0.9997
	52	99	1.3×10^{-3}	1.18	0.6322	1.91×10^{-3}	101.0	0.9961
	72	133	16×10^{-4}	1.23	0.5417	1.98×10^{-3}	133.3	0.9983

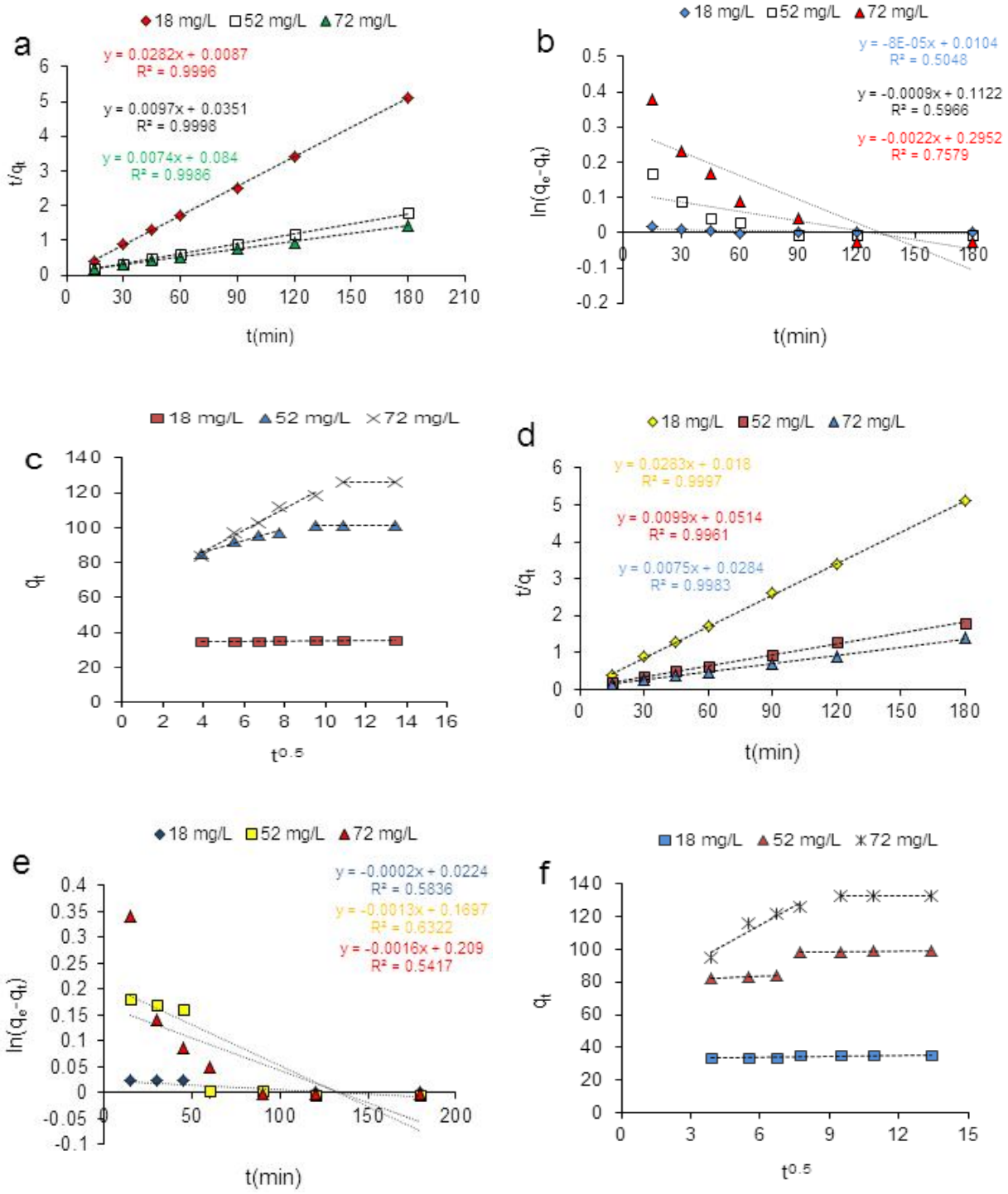

Fig. 5. (a) Pseudo-first-order, (b) pseudo-second-order, (c) intra-particle diffusion models for adsorption of CR onto the ZnO-$MgFe_2O_4$/ZnAl-LDH adsorbent, and (d) pseudo-first-order, (e) pseudo-second-order (f) intra-particle diffusion models for the ZnO-$MgFe_2O_4$/MgAl-LDH adsorbent.

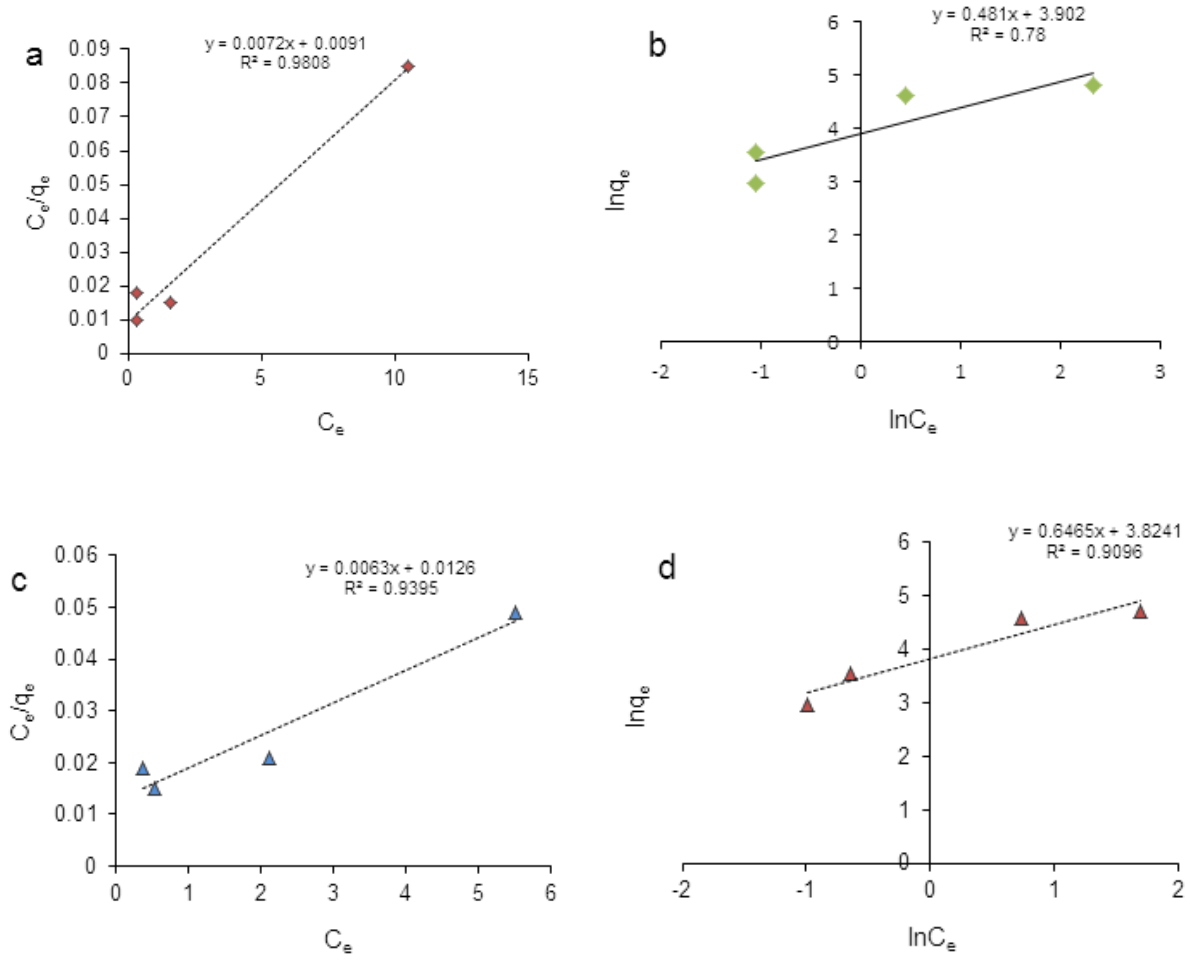

Fig. 6. Langmuir and Freundlich models for adsorption of CR dye onto the ZnO-$MgFe_2O_4$/ZnAl-LDH (a, b) and ZnO-$MgFe_2O_4$/MgAl-LDH (c, d) adsorbents.

Table 3. Parameters of Langmuir and Freundlich Models for CR Dye Removal by the ZnO-$MgFe_2O_4$/ZnAl-LDH and ZnO-$MgFe_2O_4$/MgAl-LDH Adsorbents

Sample	Langmuir isotherm				Freundlich isotherm		
	R_L	K_L	q_{max} (mg g^{-1})	R^2	K_F	n	R^2
ZnO-$MgFe_2O_4$/ZnAl-LDH	0.024	0.79	139	0.9808	49.5	2.08	0.78
ZnO-$MgFe_2O_4$/MgAl-LDH	0.037	0.5	159	0.9395	45.8	1.55	0.9096

concentration.

To find the rate controlling steps and mass transfer of CR dye onto the adsorption surface, the Weber-Morris intra-particle diffusion model was applied. For high concentration of CR dye solutions (52 and 72 mg l^{-1}), the plots were multi-linear, indicating that the external surface adsorption occurred in the first step, and in the second step intra-particle diffusion occurred [33]. For 18 mg l^{-1} of the CR dye solution, the plot was linear and did not pass through the origin, indicating that the rapid adsorption occurred within a short period of time.

The Langmuir and Freundlich isotherms were investigated for ZnO-$MgFe_2O_4$/ZnAl-LDH and ZnO-$MgFe_2O_4$/MgAl-LDH samples (Figs. 6a-d and Table 3). The results showed a higher R^2 for Langmuir compared to the Freundlich model. Therefore, adsorption process could be well fitted by the Langmuir model. The Langmuir model assumes that adsorption is limited to a monomolecular layer on the surface [34]. According to Table 3, the R_L value ($0 < R_L < 0.1$) close to zero was obtained for the ZnO-$MgFe_2O_4$/ZnAl-LDH and ZnO-$MgFe_2O_4$/MgAl-LDH samples. Therefore, the adsorption of CR dye molecules on the surface of the samples can be almost irreversible. Many researchers reported that the interaction between CR dye molecules and adsorbents might be relatively strong. Therefore, the adsorbent cannot be used several times and recovered [35]. Until now, the R_L value of ($0 < R_L < 0.1$) has been reported for the Congo red dye removal using various adsorbents [36,37].

CONCLUSIONS

In this work, two different kinds of layered double hydroxides for preparation of the ZnO-$MgFe_2O_4$/LDH composites were used. Then, the efficiency of the samples for removal of the CR dye was compared. The kinetic study of the ZnO-$MgFe_2O_4$/ZnAl-LDH, ZnO-$MgFe_2O_4$/MgAl-LDH samples revealed that the adsorption process followed the pseudo-second-order kinetic model. Adsorption isotherm for the ZnO-$MgFe_2O_4$/LDHs samples was better fitted to the Langmuir isotherm model. The adsorption capacities of the ZnAl-LDH, MgAl-LDH, ZnO-$MgFe_2O_4$/ZnAl-LDH, ZnO-$MgFe_2O_4$/MgAl-LDH and ZnO-$MgFe_2O_4$ samples were calculated 101, 101, 101, 99 and 60 mg g^{-1}, respectively. A similar efficiency was observed for the LDHs samples and LDH composites. For the ZnO-$MgFe_2O_4$/LDH samples, the R_L value close to zero was obtained. According to the results, the CR dye adsorption on the surface of the samples is predicted to be almost irreversible. However, the irreversibility of the adsorption process makes these adsorbents inefficient.

ACKNOWLEDGMENTS

We are grateful to Payame Noor University for its financial support.

REFERENCES

[1] Farias, R. S. d.; Buarque, H. L. d. B.; Cruz, M. R. d.; Cardoso, L. M. F.; Gondim, T. d. A.; Paulo, V. R. d., Adsorption of congo red dye from aqueous solution onto amino-functionalized silica gel. *Engenharia Sanitaria e Ambiental* **2018**, *23*, 1053-1060, DOI: 10.1590/s1413-41522018172982.

[2] Kumar, P.; Agnihotri, R.; Wasewar, K. L.; Uslu, H.; Yoo, C., Status of adsorptive removal of dye from textile industry effluent. *Desalin Water Treat.* **2012**, *50*, 226-244, DOI: 10.1080/19443994.2012.719472.

[3] Yagub, M. T.; Sen, T. K.; Afroze, S.; Ang, H. M., Dye and its removal from aqueous solution by adsorption: A review. *Adv. Colloid Interface Sci.* 2014, *209*, 172-184. DOI: 10.1016/j.cis.2014.04.002.

[4] Gupta, V., Application of low-cost adsorbents for dye removal-a review. *J. Environ. Manage.* **2009**, *90*, 2313-2342, DOI: 10.1016/j.jenvman.2008.11.017.

[5] Zhou, Y.; Lu, J.; Zhou, Y.; Liu, Y., Recent advances for dyes removal using novel adsorbents: A review. *Environ. Pollt.* **2019**, *252*, 352-365, DOI: 10.1016/j.envpol.2019.05.072.

[6] Daud, M.; Hai, A.; Banat, F.; Wazir, M. B.; Habib, M.; Bharath, G.; Al-Harthi, M. A., A review on the recent advances, challenges and future aspect of layered double hydroxides (LDH)-Containing hybrids as promising adsorbents for dyes removal. *J. Mol. Liq.* **2019**, *288*, 110989, DOI: 10.1016/j.molliq.2019.110989.

[7] Theiss, F. L.; Ayoko, G. A.; Frost, R. L., Synthesis of

layered double hydroxides containing Mg^{2+}, Zn^{2+}, Ca^{2+} and Al^{3+} layer cations by co-precipitation methods-A review. *Appl. Surf. Sci.* **2016**, *383*, 200-213, DOI: 10.1016/j.apsusc.2016.04.150.

[8] Yun, S. K.; Pinnavaia, T. J., Layered double hydroxides intercalated by polyoxometalate anions with Keggin (α-H2W12O406-), Dawson (α-P2W18O626-), and Finke (Co4 (H2O) 2 (PW9O34) 210-) structures. *Inorganic Chem*. **1996**, *35*, 6853-6860, DOI: 10.1021/ic960287u.

[9] Zubair, M.; Daud, M.; McKay, G.; Shehzad, F.; Al-Harthi, M. A., Recent progress in layered double hydroxides (LDH)-containing hybrids as adsorbents for water remediation. *Appl. Clay Sci.* **2017**, *143*, 279-292, DOI: 10.1016/j.clay.2017.04.002.

[10] Zare, E. N.; Motahari, A.; Sillanpää, M., Nanoadsorbents based on conducting polymer nanocomposites with main focus on polyaniline and its derivatives for removal of heavy metal ions/dyes: a review. *Environ. Res.* **2018**, *162*, 173-195, DOI: 10.1016/j.envres.2017.12.025.

[11] Lu, L.; Li, J.; Ng, D. H.; Yang, P.; Song, P.; Zuo, M., Synthesis of novel hierarchically porous Fe_3O_4@ MgAl-LDH magnetic microspheres and its superb adsorption properties of dye from water. *J. Ind. Eng. Chem.* **2017**, *46*, 315-323, DOI: 10.1016/j.jiec.2016.10.045.

[12] da Silva, L. N.; dos Santos Moraes, D.; Santos, S. C. A.; Corrêa, J. A. M., Joint synthesis of Zeolite A-LDH from mineral industry waste. *Appl. Clay Sci.* **2018**, *161*, 163-168, DOI: 10.1016/j.clay.2018.04.018.

[13] Prasad, C.; Tang, H.; Liu, Q. Q.; Zulfiqar, S.; Shah, S.; Bahadur, I., An overview of semiconductors/layered double hydroxides composites: Properties, synthesis, photocatalytic and photoelectrochemical applications. *J. Mol. Liq.* **2019**, *289*, 111114, DOI: 10.1016/j.molliq.2019.111114.

[14] Grover, A.; Mohiuddin, I.; Malik, A. K.; Aulakh, J. S.; Kim, K. -H., Zn-Al layered double hydroxides intercalated with surfactant: Synthesis and applications for efficient removal of organic dyes. *J. Clean. Prod.* **2019**, *240*, 118090, DOI: 10.1016/j.jclepro.2019.118090.

[15] Giakisikli, G.; Anthemidis, A. N., Magnetic materials as sorbents for metal/metalloid preconcentration and/or separation. A review. *Anal. Chim. Acta* **2013**, *789*, 1-16, DOI: 10.1016/j.aca.2013.04.021.

[16] Palza, H.; Delgado, K.; Govan, J., Novel magnetic $CoFe_2O_4$/layered double hydroxide nanocomposites for recoverable anionic adsorbents for water treatment. *Appl. Clay Sci.* **2019**, *183*, 105350, DOI: 10.1016/j.clay.2019.105350.

[17] Zhang, H.; Xia, B.; Wang, P.; Wang, Y.; Li, Z.; Wang, Y.; Feng, L.; Li, X.; Du, S., From waste to waste treatment: Mesoporous magnetic $NiFe_2O_4$/ ZnCuCr-layered double hydroxide composite for wastewater treatment. *J. Alloys and Compds.* **2020**, *819*, 153053, DOI: 10.1016/j.jallcom.2019.153053.

[18] Shan, R. R.; Yan, L. G.; Yang, K.; Yu, S. J.; Hao, Y. F.; Yu, H. Q.; Du, B., Magnetic Fe_3O_4/MgAl-LDH composite for effective removal of three red dyes from aqueous solution. *Chem. Eng. J.* **2014**, *252*, 38-46, DOI: 10.1016/j.cej.2014.04.105.

[19] Qiao, W.; Bai, H.; Tang, T.; Miao, J.; Yang, Q., Recovery and utilization of phosphorus in wastewater by magnetic Fe_3O_4/Zn-Al-Fe-La layered double hydroxides (LDHs). *Colloids Surf. A: Physicochem. Eng. Asp*. **2019**, *577*, 118-128, DOI: 10.1016/j.colsurfa.2019.05.046.

[20] Chen, D.; Li, Y.; Zhang, J.; Zhou, J. -Z.; Guo, Y.; Liu, H., Magnetic Fe_3O_4/ZnCr-layered double hydroxide composite with enhanced adsorption and photocatalytic activity. *Chem. Eng. J.* **2012**, *185*, 120-126, DOI: 10.1016/j.cej.2012.01.059.

[21] Xia, S. -J.; Liu, F. -X.; Ni, Z. -M.; Xue, J. -L.; Qian, P. -P., Layered double hydroxides as efficient photocatalysts for visible-light degradation of Rhodamine B. *J. Colloid Interf. Sci.* **2013**, *405*, 195-200, DOI: 10.1016/j.jcis.2013.05.064.

[22] Shi, W.; Guo, F.; Wang, H.; Liu, C.; Fu, Y.; Yuan, S.; Huang, H.; Liu, Y.; Kang, Z., Carbon dots decorated magnetic $ZnFe_2O_4$ nanoparticles with enhanced adsorption capacity for the removal of dye from aqueous solution. *Appl. Surf. Sci.* **2018**, *433*, 790-797, DOI: 10.1016/j.apsusc.2017.10.099.

[23] Zhang, H.; Chen, H.; Azat, S.; Mansurov, Z. A.; Liu, X.; Wang, J.; Su, X.; Wu, R., Super adsorption capability of rhombic dodecahedral Ca-Al layered

double oxides for Congo red removal. *Journal of Alloys Compds.* **2018**, *768*, 572-581, DOI: 10.1016/j.jallcom.2018.07.241.

[24] Yan, L. G.; Yang, K.; Shan, R. -R.; Yan, T.; Wei, J.; Yu, S. J.; Yu, H. Q.; Du, B., Kinetic, isotherm and thermodynamic investigations of phosphate adsorption onto core-shell Fe_3O_4@LDHs composites with easy magnetic separation assistance. *J. Colloid Interf. Sci.* **2015**, *448*, 508-516, DOI: 10.1016/j.jcis.2015.02.048.

[25] Khitous, M.; Salem, Z.; Halliche, D., Effect of interlayer anions on chromium removal using Mg-Al layered double hydroxides: Kinetic, equilibrium and thermodynamic studies. *Chin. J. Chem. Eng.* **2016**, *24*, 433-445, DOI: 10.1016/j.cjche.2015.11.018.

[26] Elmoubarki, R.; Mahjoubi, F. Z.; Elhalil, A.; Tounsadi, H.; Abdennouri, M.; Sadiq, M. H.; Qourzal, S.; Zouhri, A.; Barka, N., Ni/Fe and Mg/Fe layered double hydroxides and their calcined derivatives: preparation, characterization and application on textile dyes removal. *J. Mater. Res.* **2017**, *6*, 271-283, DOI: 10.1016/j.jmrt.2016.09.007.

[27] Mahjoubi, F. Z.; Khalidi, A.; Abdennouri, M.; Barka, N., Zn-Al layered double hydroxides intercalated with carbonate, nitrate, chloride and sulphate ions: Synthesis, characterisation and dye removal properties. *J. Taibah Univ. Sci.,* **2017**, *11*, 90-100. DOI: 10.1016/j.jtusci.2015.10.007.

[28] López, T.; Bosch, P.; Asomoza, M.; Gómez, R.; Ramos, E., DTA-TGA and FTIR spectroscopies of sol-gel hydrotalcites: aluminum source effect on physicochemical properties. *Mater. Lett.,* **1997**, *31*, 311-316. DOI: 10.1016/S0167-577X(96)00296-0.

[29] Zhang, Y.; Wang, L.; Zou, L.; Xue, D., Crystallization behaviors of hexagonal nanoplatelet MgAl-CO_3 layered double hydroxide. *J. Cryst. Growth,* **2010**, *312*, 3367-3372. DOI: 10.1016/j.jcrysgro.2009.10.068

[30] Alghamdi, A. A.; Al-Odayni, A. B.; Saeed, W. S.; Al-Kahtani, A.; Alharthi, F. A.; Aouak, T., Efficient adsorption of lead(II) from aqueous phase solutions using polypyrrole-based activated carbon. *Materials (Basel).* **2019**, *12*, 2020. DOI: 10.3390/ma12122020.

[31] Jabar, J. M.; Odusote, Y. A.; Alabi, K. A.; Ahmed, I. B., Kinetics and mechanisms of congo-red dye removal from aqueous solution using activated Moringa oleifera seed coat as adsorbent. *Appl. Water Sci.,* **2020**, *10*, 136. DOI:10.1007/s13201-020-01221-3.

[32] Taher, T.; Rohendi, D.; Mohadi, R.; Lesbani, A., Congo red dye removal from aqueous solution by acid-activated bentonite from sarolangun: kinetic, equilibrium, and thermodynamic studies. *Arab. J. Basic Appl. Sci.,* **2019**, *26*, 125-136. DOI: 10.1080/25765299.2019.1576274.

[33] Fierro, V.; Torné-Fernández, V.; Montané, D.; Celzard, A., Adsorption of phenol onto activated carbons having different textural and surface properties. *Microporous Mesoporous Mater.,* **2008**, *111*, 276-84. DOI: 10.1016/j.micromeso.2007.08.002.

[34] Saadi, R.; Saadi, Z.; Fazaeli, R.; Fard, N. E., Monolayer and multilayer adsorption isotherm models for sorption from aqueous media. *Korean J. Chem. Eng.* **2015**, *32*, 787-99. DOI: 10.1007/s11814-015-0053-7.

[35] Baghban, A.; Jabbari, M.; Rahimpour, E., Fe_3O_4@ Polydopamine core-shell nanocomposite as a sorbent for efficient removal of rhodamine B from aqueous solutions: Kinetic and equilibrium studies. *Iran. J. Chem. Chem. Eng.* **2018**, *37*, 17-28. DOI: 10.30492/JCCE.2018.26374.

[36] Zhou, Y.; Ge, L.; Fan, N.; Xia, M., Adsorption of Congo red from aqueous solution onto shrimp shell powder. *Adsorp. Sci. Technol.,* **2018**, *36*, 1310-1330. DOI: 10.1177/0263617418768945.

[37] Ojedokun, A. T.; Bello, O. S., Kinetic modeling of liquid-phase adsorption of Congo red dye using guava leaf-based activated carbon. *Appl. Water Sci.,* **2017**, *7*, 1965-1977. DOI: 10.1007/s 13201-015-0375-y.

[38] Ahmed, I.; Gasser, M., Adsorption study of anionic reactive dye from aqueous solution to Mg-Fe-CO_3 layered double hydroxide (LDH). *Appl. Surf. Sci.* **2012**, *259*, 650-656, DOI: 10.1016/j.apsusc.2012.07.092.

[39] Bharali, D.; Deka, R. C., Preferential adsorption of various anionic and cationic dyes from aqueous solution over ternary CuMgAl layered double hydroxide. *Colloids Surf. A: Physicochem.*

Eng. Asp. **2017**, *525*, 64-76, DOI: 10.1016/ j.colsurfa.2017.04.060.

[40] Dao, T. U. T.; Nguyen, H. T. T.; Sy, D. T.; Nguyen, K. H.; Nguyen, A. T.; Nguyen, T. T.; Nguyen, T. D., In Adsorption isotherms and kinetic models for congo red adsorption on Ca-Al layer double hydroxide adsorbent, *Solid State Phenom.* **2019**, *298*, 128-132, DOI: 10.4028/ www.scientific.net/SSP.298.128.

[41] Wang, Q.; Tang, A.; Zhong, L.; Wen, X.; Yan, P.; Wang, J., Amino-modified γ-Fe_2O_3/sepiolite composite with rod-like morphology for magnetic separation removal of Congo red dye from aqueous solution. *Powder Technol.* **2018**, *339*, 872-881, DOI: 10.1016/j.powtec.2018.08.055.

[42] Zhu, H. Y.; Fu, Y. Q.; Jiang, R.; Jiang, J. -H.; Xiao, L.; Zeng, G. M.; Zhao, S. L.; Wang, Y., Adsorption removal of congo red onto magnetic cellulose/Fe_3O_4/ activated carbon composite: Equilibrium, kinetic and thermodynamic studies. *Chem. Eng.* **2011**, *173*, 494-502, DOI: 10.1016/ j.cej.2011.08.020.